A density matrix renormalization group study of low-energy excitations and low-temperature properties of alternating spin systems

1997 J. Phys.: Condens. Matter 9 8707

(http://iopscience.iop.org/0953-8984/9/41/016)

J. Phys.: Condens. Matter **9** (1997) 8707–8726. Printed in the UK PII: S0953-8984(97)83462-5

A density matrix renormalization group study of low-energy excitations and low-temperature properties of alternating spin systems

Swapan K Pati†, S Ramasesha†‡ and Diptiman Sen‡§

† Solid State and Structural Chemistry Unit, Indian Institute of Science, Bangalore 560012, India
‡ Jawaharlal Nehru Centre for Advanced Scientific Research, Jakkur Campus, Bangalore 560064, India
§ Centre for Theoretical Studies, Indian Institute of Science, Bangalore 560012, India

Received 15 April 1997, in final form 10 July 1997

Abstract. We use the density matrix renormalization group (DMRG) method to study the ground and low-lying excited states of three kinds of uniform and dimerized alternating spin chain. The DMRG procedure is also employed to obtain low-temperature thermodynamic properties of these systems. We consider a $2N$-site system with spins s_1 and s_2 alternating from site to site and interacting via a Heisenberg antiferromagnetic exchange. The three systems studied correspond to (s_1, s_2) being equal to $(1, \frac{1}{2})$, $(\frac{3}{2}, \frac{1}{2})$ and $(\frac{3}{2}, 1)$; all of them have very similar properties. The ground state is found to be ferrimagnetic with total spin $s_G = N(s_1 - s_2)$. We find that there is a gapless excitation to a state with spin $s_G - 1$, and a gapped excitation to a state with spin $s_G + 1$. The DMRG analysis shows that the chain is susceptible to a conditional spin–Peierls instability. Furthermore, our studies of the magnetization, magnetic susceptibility χ and specific heat show strong magnetic field dependences. The product χT shows a minimum as a function of temperature T at low magnetic fields; the minimum vanishes at high magnetic fields. This low-field behaviour is in agreement with earlier experimental observations. The specific heat shows a maximum as a function of temperature, and the height of the maximum increases sharply at high magnetic fields. Although all three systems show qualitatively similar behaviour, there are some notable quantitative differences between the systems in which the site spin difference, $|s_1 - s_2|$, is large and small respectively.

1. Introduction

There have been a number of experimental efforts over the last few years to synthesize molecular systems showing spontaneous magnetization [1–3]. These studies have led to the recent realization of systems such as NPNN (*para*-nitrophenyl nitronyl nitroxide) and C_{60}-TDAE (tetrakis dimethyl amino ethylene) which show ferromagnetic-to-paramagnetic transitions at low temperatures. There also exist theoretical models [4, 5] that predict ferrimagnetism in organic polymer systems, but a truly extended organic ferrimagnet has not been synthesized, although an oligomer with a ground-state spin of $S = 9$ is now known. On the inorganic front, pursuit of molecular magnetism has been vigorous, and there has been success in the synthesis of molecular systems showing spontaneous magnetization at low temperatures [6, 7]. These are quasi-one-dimensional bimetallic molecular magnets in which each unit cell contains two spins with different spin values [7]. These systems contain two transition metal ions per unit cell, with the general formula $ACu(pbaOH)(H_2O)_3{\cdot}2H_2O$, where pbaOH is 2-hydroxo-1, 3-propylenebis(oxamato) and A = Mn, Fe, Co, Ni, and they

0953-8984/97/418707+20$19.50

belong to the alternating or mixed spin-chain family [8]. These alternating spin compounds have been seen to exhibit ferrimagnetic behaviour. It has been possible to vary the spin at each site from low values where quantum effects dominate to large values which are almost classical.

There have been a number of theoretical investigations of quantum ferrimagnetic systems in recent years [9, 10]. However, these models consider complicated multispin interactions, while very little is known about the simple Heisenberg model with purely quadratic interactions. There have been some analytical and numerical studies of an alternating spin-1/spin-$\frac{1}{2}$ system [11], a more general alternating spin chain [12], and a detailed spin-wave analysis followed by a DMRG study [13] corresponding to the Cu–Ni bimetallic chain with the simple Heisenberg model. These studies confirm that these ferrimagnetic systems can be accurately described by a pure Heisenberg spin model.

Theoretical studies of alternating spin systems have so far concentrated on the spin-1/spin-$\frac{1}{2}$ bimetallic chains; further, the thermodynamic properties have not been explored in detail. The thermodynamic behaviour of these alternating spin compounds is very interesting [8, 14]. In very low magnetic fields, these systems show one-dimensional ferrimagnetic behaviour. The χT versus T (where χ is the magnetic susceptibility and T the temperature) plots show a rounded minimum. As the temperature is increased, χT decreases sharply, and then goes through a minimum before increasing gradually. The temperature at which this minimum occurs differs from system to system and depends on the site spins of the chain. The variation of the field-induced magnetization with temperature is also interesting as the ground state is a magnetic state. At low magnetic fields, the magnetization decreases with increasing temperature at low temperatures. However, at moderate magnetic fields, with increase in temperature, the magnetization slowly increases, shows a broad peak and then decreases. Such a behaviour has been studied theoretically by us for the spin-1/spin-$\frac{1}{2}$ system [13].

These interesting observations have motivated us to study ferrimagnetic systems with arbitrary spins s_1 and s_2 alternating from site to site. It would be quite interesting to know the thermodynamic properties of these systems with varying s_1 and s_2. In the previous paper, we predicted some interesting features of the thermodynamic properties of the spin-1/spin-$\frac{1}{2}$ system at high magnetic fields. We focus on the high-field behaviour of the general ferrimagnetic chains to find whether the observed properties are generic to these systems or are dependent on specific s_1- and s_2-values.

In this paper, we study the low-lying excited states and low-temperature properties of the spin-$\frac{3}{2}$/spin-1 and spin-$\frac{3}{2}$/spin-$\frac{1}{2}$ chains and rings, and compare them with those of the corresponding spin-1/spin-$\frac{1}{2}$ systems. We have employed the density matrix renormalization group (DMRG) method which has proved to be the best numerical tool for low-dimensional spin systems in recent years [15]. The ground-state energy per site, the spin excitation gap and the two-spin correlation functions obtained from this method have been found to be accurate to several decimal places [16–18] when compared with Bethe *ansatz* results (where possible) and exact-diagonalization results for small systems. In the DMRG method, spin-parity symmetry can be used to characterize the spin states along with the S^z_{tot} as the good quantum numbers. The DMRG calculations have been carried out on chains and rings with alternate spin-s_1/spin-s_2 sites, with s_1 fixed at $\frac{3}{2}$ and s_2 being 1 or $\frac{1}{2}$. Studies of the ground state and low-lying excited states are reported in detail and compared with those of $s_1 = 1$ and $s_2 = \frac{1}{2}$ system. Furthermore, by resorting to a full diagonalization of the DMRG Hamiltonian matrix in different S_z-sectors, we have also obtained the low-temperature thermodynamic properties of these systems. The thermodynamic properties that we discuss will include the low- and high-field magnetization, magnetic susceptibility and

specific heat, all at low temperatures.

The paper is organized as follows. In section 2, we present the properties of the ground and low-lying excited states and compare them with the results of spin-wave theory. In section 3, we discuss the low-temperature thermodynamic properties of the systems. We summarize our results in the last section.

2. The ground state and the excitation spectrum

We start our discussion with the Hamiltonian for a chain with spins s_1 and s_2 on alternating sites (with $s_1 > s_2$, without loss of generality):

$$H = J \sum_n [(1+\delta)\boldsymbol{S}_{1,n} \cdot \boldsymbol{S}_{2,n} + (1-\delta)\boldsymbol{S}_{2,n} \cdot \boldsymbol{S}_{1,n+1}] \tag{1}$$

where the total number of sites is $2N$ and the sum is over the total number of unit cells N. $\boldsymbol{S}_{i,n}$ corresponds to the spin operator for the site spin s_i in the nth unit cell. The exchange integral J is taken to be positive for all of our calculations; δ is the dimerization parameter and it lies in the range $[0, 1]$.

2.1. Summary of the results from spin-wave theory

Before describing our numerical results, we briefly summarize the results of a spin-wave analysis for the purposes of comparison [13]. We will first state the results for $\delta = 0$. According to spin-wave theory, the ground state has total spin $s_G = N(s_1 - s_2)$. Let us define a function

$$\omega(k) = J\sqrt{(s_1 - s_2)^2 + 4s_1 s_2 \sin^2(k/2)} \tag{2}$$

where k denotes the wavenumber. Then the ground-state energy per site is given by

$$\varepsilon_0 = \frac{E_0}{2N} = -Js_1 s_2 + \frac{1}{2}\int_0^\pi \frac{\mathrm{d}k}{\pi}\,[-J(s_1 + s_2) + \omega(k)]. \tag{3}$$

The lowest branch of excitations is to states with spin $s = s_G - 1$, with the dispersion

$$\omega_1(k) = J(-s_1 + s_2) + \omega(k). \tag{4}$$

The gap vanishes at $k = 0$. There is a gapped branch of excitations to states with spin $s = s_G + 1$, with the dispersion

$$\omega_2(k) = J(s_1 - s_2) + \omega(k). \tag{5}$$

The minimum gap occurs at $k = 0$ and is given by $\Delta = 2J(s_1 - s_2)$. In the ground state with $S_z = s_G$, the sublattice magnetizations are given by the expectation values

$$\begin{aligned} \langle S^z_{1,n}\rangle &= \left(s_1 + \frac{1}{2}\right) - \frac{1}{2}\int_0^\pi \frac{\mathrm{d}k}{\pi}\,\frac{J(s_1 + s_2)}{\omega(k)} \\ \langle S^z_{2,n}\rangle &= s_1 - s_2 - \langle S^z_{1,n}\rangle. \end{aligned} \tag{6}$$

The fluctuations in the various two-spin correlation functions decay exponentially with distance; the inverse correlation length is given by $\xi^{-1} = \ln(s_1/s_2)$. The results with dimerization ($\delta > 0$) are very similar. In fact, within spin-wave theory, the minimum gap Δ to states with spin $s = s_G + 1$ is independent of δ.

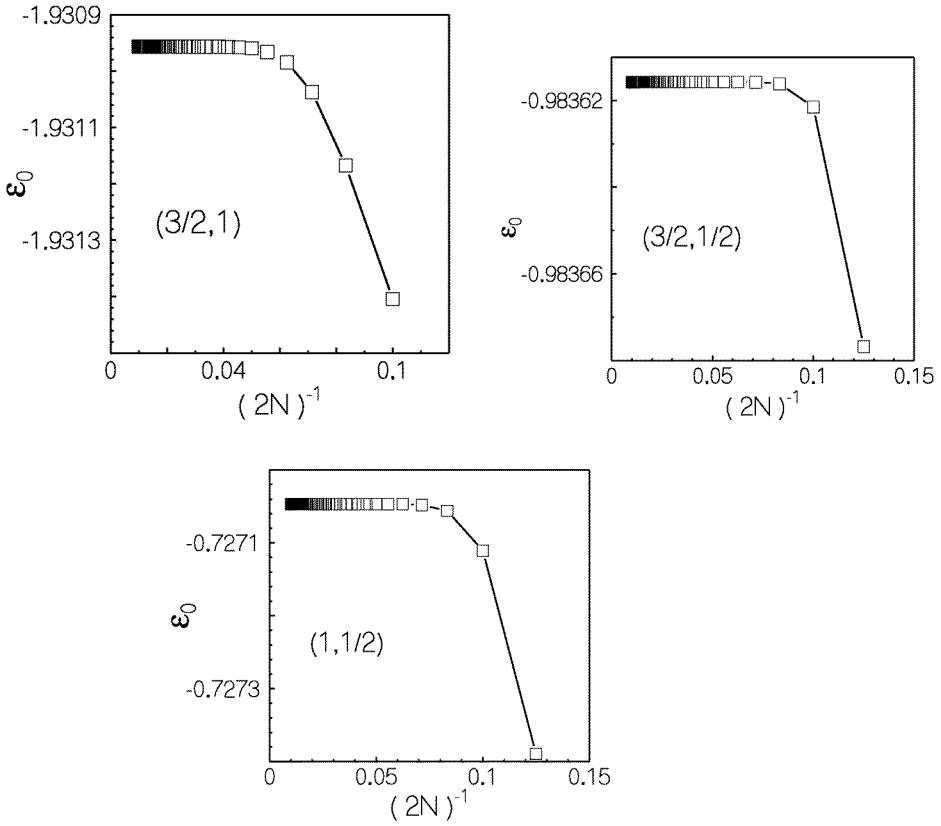

Figure 1. Extrapolations of the ground-state energy per site (ε_0), in units of J, as functions of the inverse system size.

2.2. Results from DMRG studies

We have studied the system defined by equation (1) both with and without dimerization, $\delta \neq 0$ and $\delta = 0$ respectively. We study alternating spin-$\frac{3}{2}$/spin-1 (hereafter designated as $(\frac{3}{2}, 1)$) and spin-$\frac{3}{2}$/spin-$\frac{1}{2}$ (to be called $(\frac{3}{2}, \frac{1}{2})$) chains with open boundary conditions for the Hamiltonian (1) by employing the DMRG method. We compute the ground-state properties for both of the systems by studying chains of up to 80 to 100 sites. The number of dominant density matrix eigenstates, m, that we have retained at each DMRG iteration also varies between 80 to 100 for both of the systems. With the increase of the Fock space dimensionality of the site spins, we increase m to obtain more accurate results. We follow the usual steps for the 'infinite-system' DMRG method discussed in earlier papers [15, 17, 18], except that the alternating chains studied here do not have symmetric left and right halves; hence the density matrices for these two halves have to be separately constructed at every iteration of the calculations. At each stage, we target the lowest energy state in a given S_z-sector of the chain, and we then carry out the partial trace over the left (right) half of the chain to obtain the density matrix of the right (left) half. We study sectors of the chain with a range of values of S_z, and we compute the partial trace and the density matrix from each of these. For instance, for the ground state of $2N$ sites, we study all $2s_G + 1$ values of S_z, where $s_G = N(s_1 - s_2)$. Finally, we have verified the convergence

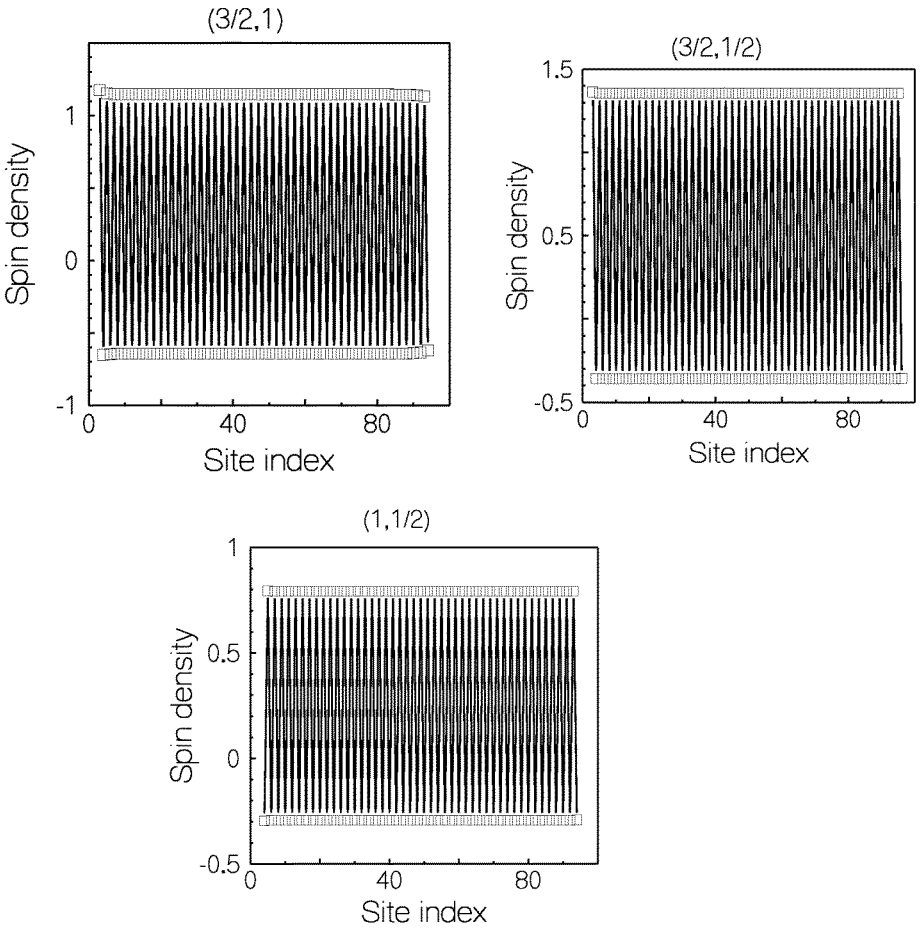

Figure 2. Expectation values of the z-components of the two spins versus the unit-cell index n. The upper and lower points are for the spin-s_1 and the spin-s_2 sites respectively.

of our results by varying the values of m and the system size.

The ground states of both of the systems lie in the $S_z = N(s_1 - s_2)$ sector, as verified from extensive checks carried out by obtaining the low-energy eigenstates in different S_z-sectors of a 20-site chain. A state corresponding to the lowest energy in $S_z = N(s_1 - s_2)$ is found in all subspaces with $|S_z| \leqslant N(s_1 - s_2)$, and is absent in subspaces with $|S_z| > N(s_1 - s_2)$. This shows that the spin in the ground state is $s_G = N(s_1 - s_2)$. (Actually, the lowest energy states in the different S_z-sectors are found to be degenerate only up to $10^{-5}J$. Such small errors are negligible for studying the thermodynamics at temperatures larger than, say, $10^{-2}J$.)

In a previous paper, we studied the alternating spin chain made up of spin-1 and spin-$\frac{1}{2}$ (hereafter referred to as $(1, \frac{1}{2})$) at alternate sites [13]. We compare here the results for all three systems, namely, $(\frac{3}{2}, 1)$, $(\frac{3}{2}, 1/2)$ and $(1, \frac{1}{2})$ spin systems. In figure 1, we show the extrapolation of the energy per site as a function of inverse system size for all three systems. The ground-state energy per site ε_0 extrapolates to $-1.930\,96J$ for the $(\frac{3}{2}, 1)$ system, to $-0.983\,62J$ for $(\frac{3}{2}, \frac{1}{2})$, and to $-0.727\,04J$ for $(1, \frac{1}{2})$. The spin-wave analysis

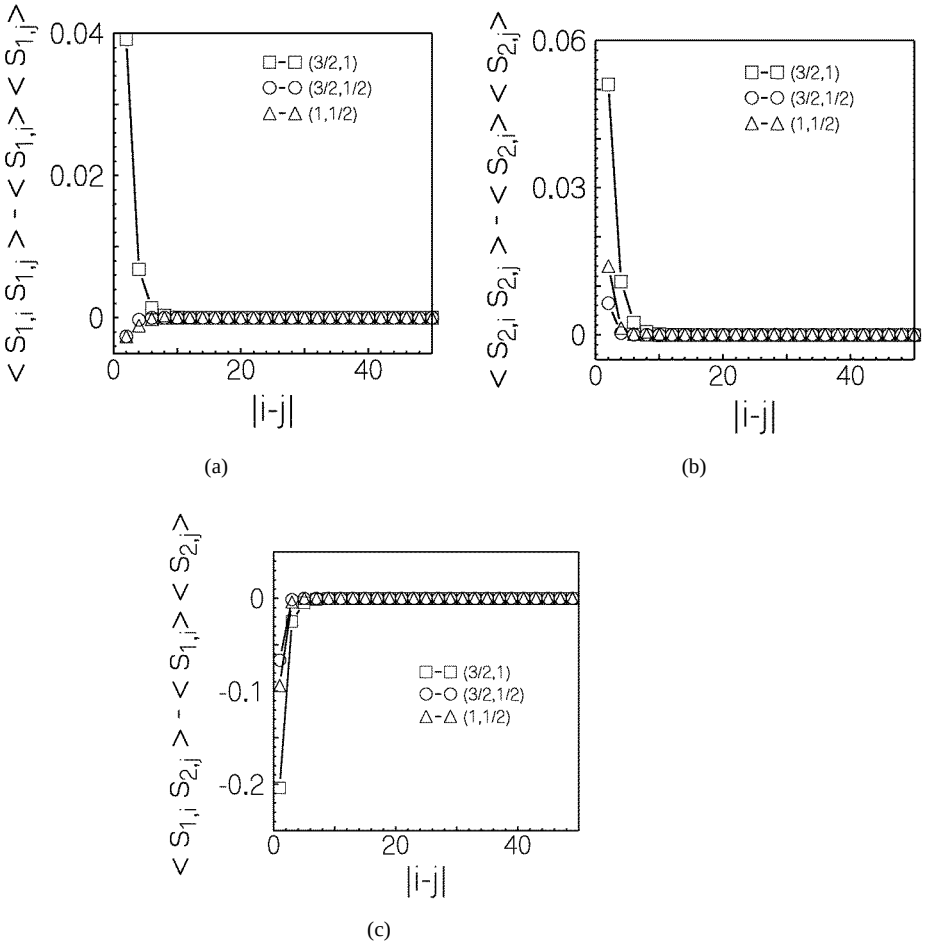

Figure 3. Subtracted two-spin correlation functions as functions of the distance between the two spins. (a) Spin-s_1–spin-s_1 correlations, (b) spin-s_2–spin-s_2 correlations, and (c) spin-s_1–spin-s_2 correlations. In each panel, squares correspond to $(\frac{3}{2}, 1)$), circles to $(\frac{3}{2}, \frac{1}{2})$ and triangles to $(1, \frac{1}{2})$ systems.

gives the values $-1.914J$ for $(\frac{3}{2}, 1)$, $-0.979J$ for $(\frac{3}{2}, \frac{1}{2})$ and $-0.718J$ for $(1, \frac{1}{2})$ which are all higher than the DMRG values. It is interesting to note that, in the alternating spin cases, the energy per site lies in between the values for the pure spin-s_1 uniform chain and the pure spin-s_2 uniform chain.

In figure 2, we show the expectation value of site spin operator $S^z_{i,n}$ (spin density) at all of the sites for the $(\frac{3}{2}, 1)$, $(\frac{3}{2}, \frac{1}{2})$ and $(1, \frac{1}{2})$ chains. The spin densities are uniform on each of the sublattices in the chain for all three systems. For the $(\frac{3}{2}, 1)$ chain, the spin density at a spin-$\frac{3}{2}$ site is 1.144 27 (the classical value is $\frac{3}{2}$), while at a spin-1 site it is $-0.644\,27$ (classical value 1). For the $(\frac{3}{2}, \frac{1}{2})$ case, the spin density at a spin-$\frac{3}{2}$ site is 1.357 42 and at a spin-$\frac{1}{2}$ site it is $-0.357\,42$. For the $(1, \frac{1}{2})$ case, the value at a spin-1 site is 0.792 48 and at a spin-$\frac{1}{2}$ site it is $-0.292\,48$. These can be compared with the spin-wave values of 1.040 and -0.540; 1.314 and -0.314; and 0.695 and -0.195 for the spin-s_1 and spin-s_2 sites of the $(\frac{3}{2}, 1)$; $(\frac{3}{2}, \frac{1}{2})$; and $(1, \frac{1}{2})$ systems respectively. We note that the spin-wave analysis

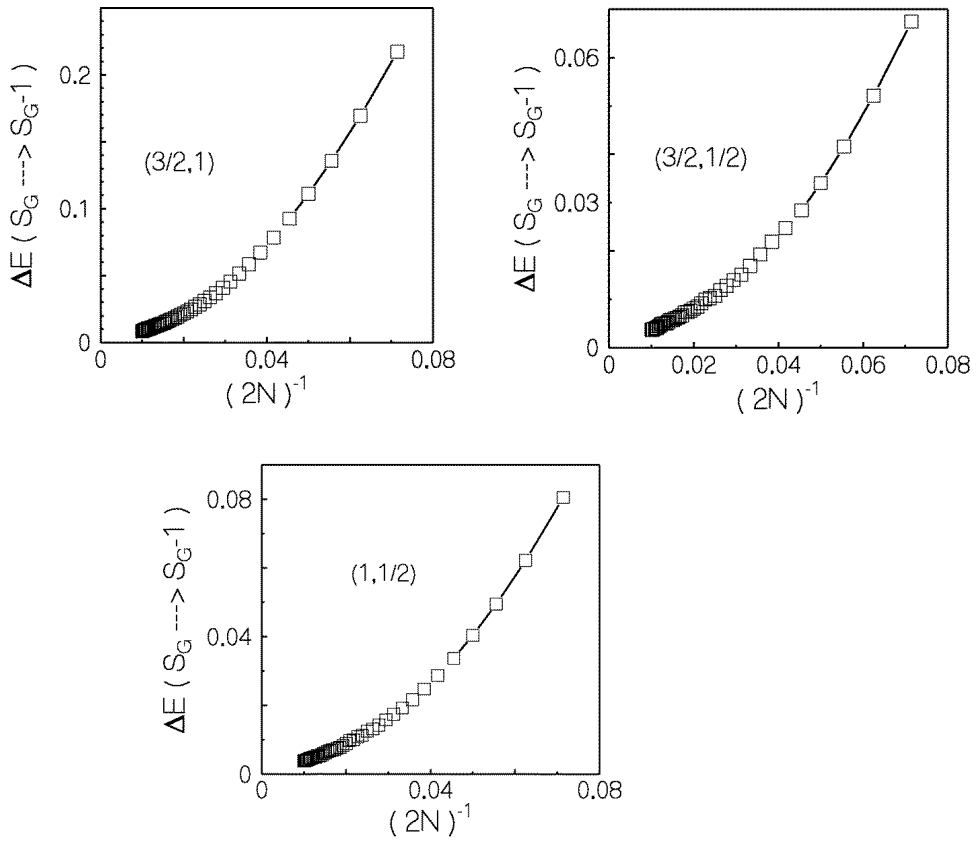

Figure 4. Energy differences (in units of J) between the ground state and the lowest energy state with spin $s = s_G - 1$ as functions of the inverse system size. s_G is the total spin of the ground state.

overestimates the quantum fluctuations in the case of systems with small site spin values. We also notice that there is a greater quantum fluctuation when the difference in site spin $|s_1 - s_2|$ is larger. This is also seen in spin-wave theory. The spin-density distribution in an alternating (s_1, s_2) chain behaves more like that in a ferromagnetic chain rather than like an antiferromagnet, with the net spin of each unit cell perfectly aligned (but with small quantum fluctuations on the individual sublattices). In a ferromagnetic ground state, the spin density at each site has the classical value appropriate to the site spin, whereas for an antiferromagnet, this averages out to zero at each site, as the ground state is nonmagnetic. From this viewpoint, the ferrimagnet is similar to a ferromagnet and is quite unlike an antiferromagnet. The spin-wave analysis also yields the same physical picture.

Because of the alternation of spin-s_1 and spin-s_2 sites along the chain, one has to distinguish between three different types of pair correlation, namely, $\langle S^z_{1,0} S^z_{1,n} \rangle$, $\langle S^z_{2,0} S^z_{2,n} \rangle$ and $\langle S^z_{1,0} S^z_{2,n} \rangle$. We calculate all three correlation functions with the mean values subtracted out, since the mean values are nonzero in all of these three systems unlike in pure antiferromagnetic spin chains. In the DMRG procedure, we have computed these correlation functions from the sites inserted at the last iteration, to minimize numerical errors. In figure 3, we plot the two-spin correlation functions in the ground state as a function of the distance

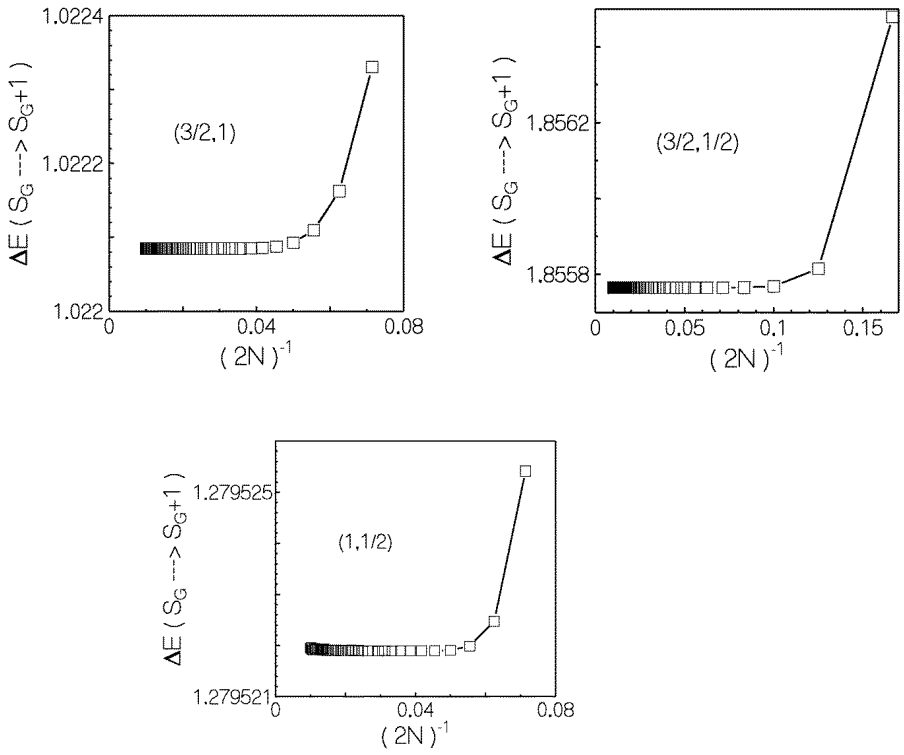

Figure 5. Excitation gaps (in units of J) from the ground state (spin $s = s_G$) to the state with spin $s = s_G + 1$ as functions of the inverse system size.

between the spins for an open chain of 100 sites for all three cases. All three correlation functions decay rapidly with distance for each of the three systems. From the figure it is clear that, except for the $\langle S^z_{1,0} S^z_{2,n} \rangle$ correlation, all other correlations are almost zero even for the shortest possible distances. The $\langle S^z_{1,0} S^z_{2,n} \rangle$ correlation has an appreciable value (-0.2 for $(\frac{3}{2}, 1)$, -0.07 for $(\frac{3}{2}, \frac{1}{2})$ and -0.094 for $(1, \frac{1}{2})$) only for the nearest neighbours. This rapid decay of the correlation functions makes it difficult to find the exact correlation length ξ for a lattice model, although it is clear that ξ is very small (less than one unit cell) for the $(\frac{3}{2}, \frac{1}{2})$ and $(1, \frac{1}{2})$ cases, and a little greater ($1 < \xi < 2$) for the $(\frac{3}{2}, 1)$ system. Spin-wave theory gives $\xi = 2.47$ for $(\frac{3}{2}, 1)$, $\xi = 0.91$ for $(\frac{3}{2}, \frac{1}{2})$, and $\xi = 1.44$ for $(1, \frac{1}{2})$ cases. (We should remark here that our ξ is not to be confused with the conventional definition of the correlation length; the latter is actually infinite in these systems due to the long-range ferrimagnetic order.)

The lowest spin excitation of all of the three chains is to a state with $s = s_G - 1$. To study this state, we target the second state in the $S_z = s_G - 1$ sector of the chain. To confirm that this state is an $s = s_G - 1$ state, we have computed the second state in the $S_z = 0$ sector and find that it also has the same energy. However, the corresponding state is absent in S_z-sectors with $|S_z| > s_G - 1$. Besides, from exact diagonalization of all of the states of all of the $s_1 - s_2$ alternating spin chains with eight sites, we find that the energy orderings of the states is such that the lowest excitation is to a state with spin $s = s_G - 1$. We have obtained the excitation gaps for all of the three alternating spin chains in the limit

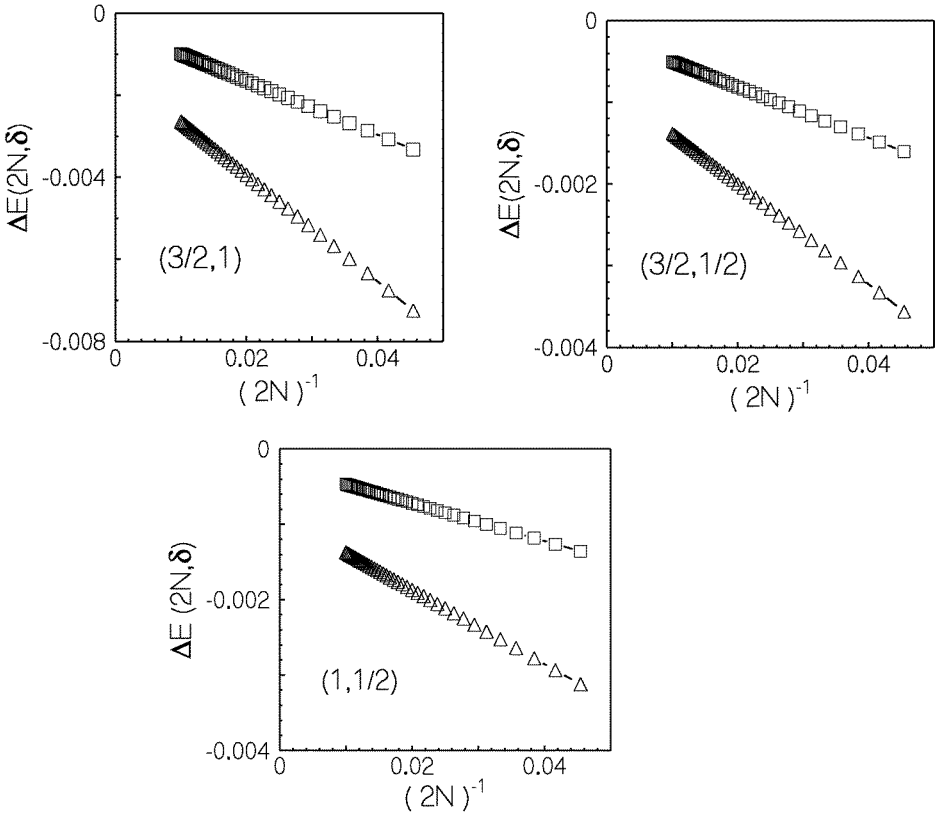

Figure 6. Gains in magnetic energy $\Delta E(2N, \delta)$ (in units of J) associated with dimerization versus the inverse system size for two different values of the dimerization δ: $\delta = 0.025$ (squares) and $\delta = 0.05$ (triangles).

of infinite chain length by extrapolating from the plot of spin gap versus the inverse of the chain length (figure 4). We find that this excitation is gapless in the infinite-chain limit for all three cases.

To characterize the lowest spin excitations completely, we also have computed the energy of the $s = s_G + 1$ state by targeting the lowest state in the $S_z = s_G + 1$ sector. In figure 5, we plot the excitation gaps to the $s = s_G + 1$ state from the ground state for all three systems as a function of the inverse of the chain length. The gap saturates to a finite value of $(1.0221 \pm 0.0001)J$ for the $(\frac{3}{2}, 1)$ case, $(1.8558 \pm 0.0001)J$ for $(\frac{3}{2}, \frac{1}{2})$, and $(1.2795 \pm 0.0001)J$ for $(1, \frac{1}{2})$. It appears that the gap is also higher when the difference in site spins $|s_1 - s_2|$, is larger. The site spin-density expectation values computed in this state for all three cases are found to be uniform (i.e. independent of the site) on each of the sublattices. This leads us to believe that this excitation cannot be characterized as the states of a magnon confined in a box, as has been observed for a spin-1 chain in the Haldane phase [16].

Earlier studies on pure spin-1 and pure spin-$\frac{1}{2}$ chains [19] have revealed that with the alternation δ in the exchange parameter, the half-odd-integer spin chain will have an unconditional spin–Peierls transition, while for integer spin chains, the transition is conditional. This conclusion has been drawn from the fact that, with the inclusion of δ, the

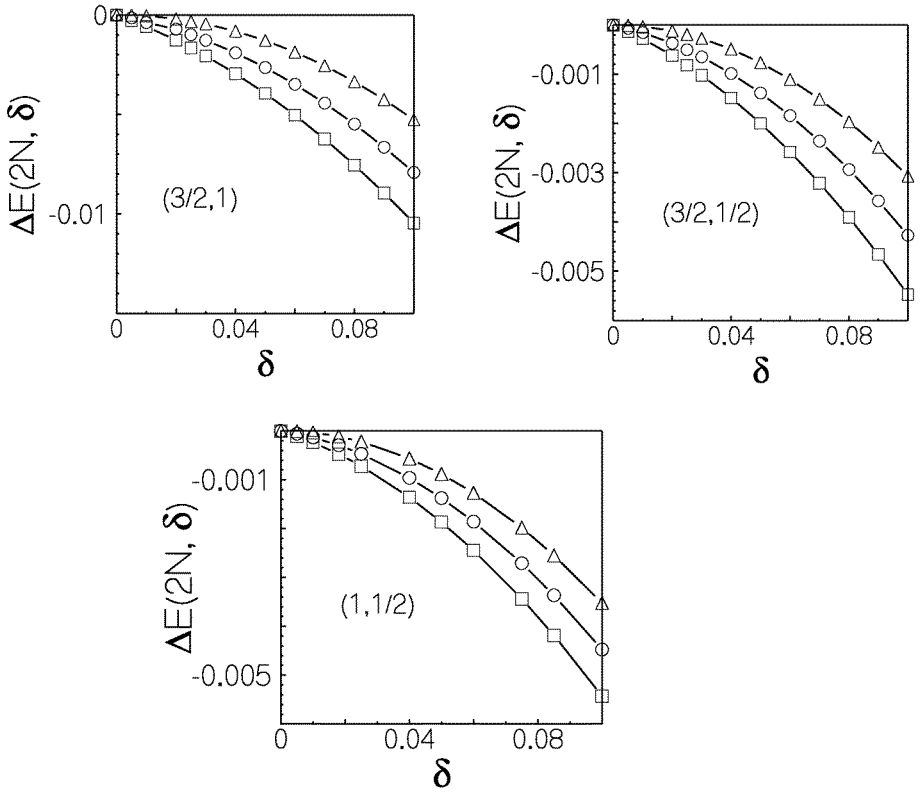

Figure 7. Magnetic energy gains (in units of J) as functions of the dimerization parameter δ for different system sizes. In the panels, $2N = 50$ (squares), $2N = 100$ (circles) and extrapolated values with $N \to \infty$ (triangles) are shown.

magnetic energy gain ΔE can be defined as

$$\Delta E(2N, \delta) = \frac{1}{2N}[E(2N, \delta) - E(2N, 0)] \tag{7}$$

where $E(2N, \delta)$ is the ground-state energy of the $2N$-site system with an alternation δ in the exchange integral, and $E(2N, 0)$ is the ground-state energy of the uniform chain of $2N$ sites. For the pure spin chain, if we assume that ΔE varies as δ^{α} for small δ, we find that $\alpha < 2$ for the half-odd-integer spin chains and $\alpha = 2$ for the integer spin chains [19]. Now if we consider the spins to lie on the sites of a deformable lattice, the value of δ is proportional to the local deformation from the equilibrium lattice configuration, while the elastic energy cost of the deformation is proportional to the square of the deformation, and hence to δ^2. Thus, for a half-odd-integer spin chain, the spin stabilization energy always overcomes the lattice elastic energy for small enough values of δ, leading to a spontaneous spin–Peierls distortion in the ground state. For the integer spin case, however, it depends on the relative magnitudes of the spin exchange and the lattice stiffness; hence the occurrence of a spin–Peierls distortion is *conditional*.

We have used DMRG calculations to extend these studies to the alternating spin systems. We obtain $\Delta E(2N, \delta)$, for small values of δ for all three alternating spin chains. To determine the exact functional form of the magnetic energy gain, we varied the chain length

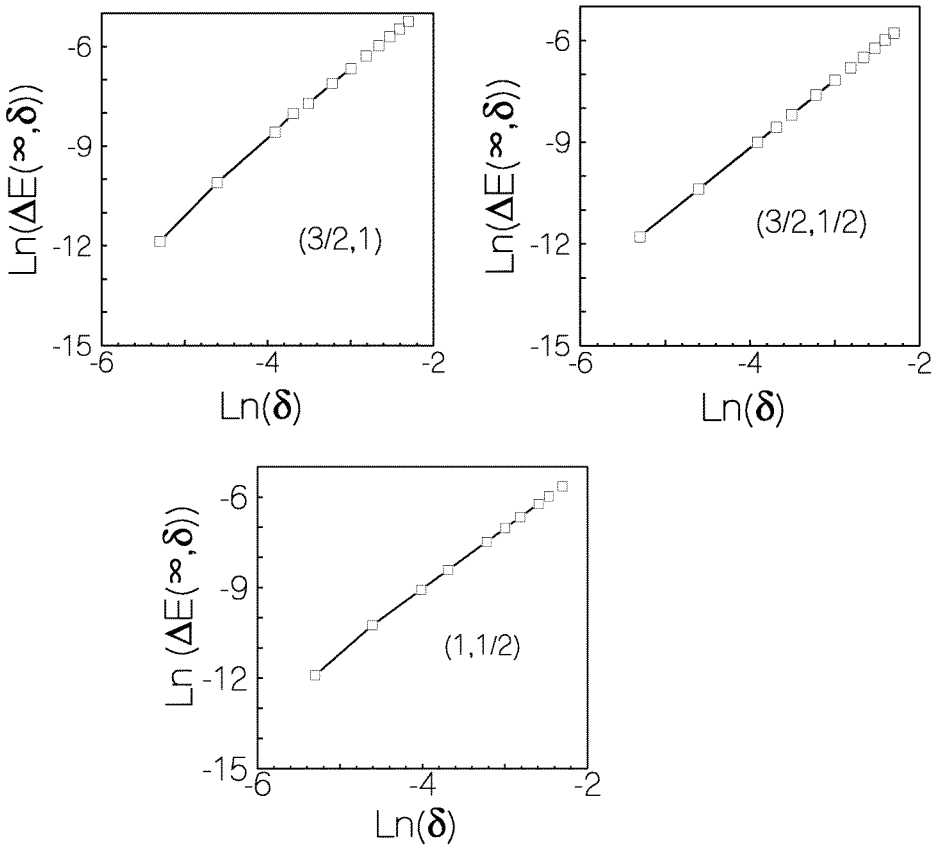

Figure 8. Log–log plots of the extrapolated magnetic energy gain (in units of J) for infinite system size and dimerization parameter δ. Interestingly, the slope is found to be 2.00 ± 0.01 for all three systems.

from 50 sites to 100 sites and also m (the number of states retained in each DMRG iteration) from 80 to 100 to check the convergence of ΔE with chain length. We note that as we approach the classical spin limit, the convergence is reached more quickly. The dependence of $\Delta E(2N, \delta)$ on $1/2N$ is linear for all three cases for the δ-values that we have studied. Figure 6 gives a sample variation of $\Delta E(2N, \delta)$ with $1/2N$ for all of the systems that we have studied. This allows us to extrapolate $\Delta E(2N, \delta)$ to the infinite-chain limit reliably for all of the cases. In figure 7, we show the plot of $\Delta E(2N, \delta)$ versus δ for finite $2N$-values and also the extrapolated infinite-chain values for all three systems. We see that there is a gain in magnetic energy upon dimerization even in the infinite-chain limit for all of the systems. To obtain the exponent α, we plot $\ln \Delta E(2N, \delta)$ versus $\ln \delta$ for the infinite chain (figure 8). From this figure, we find that in the alternating spin case, for the infinite chain $\Delta E \approx \delta^{2.00 \pm 0.01}$ for all three cases. Thus the spin–Peierls transition appears to be close to being conditional in these systems. The magnetic energy gain per site for finite chains is larger than that of the infinite chain for any value of δ (figure 7). It is possible that the distortion in a *finite* chain is unconditional while that of the infinite chain is conditional for ferrimagnetic systems.

We have also studied the spin excitations in the dimerized alternating (s_1, s_2) chains,

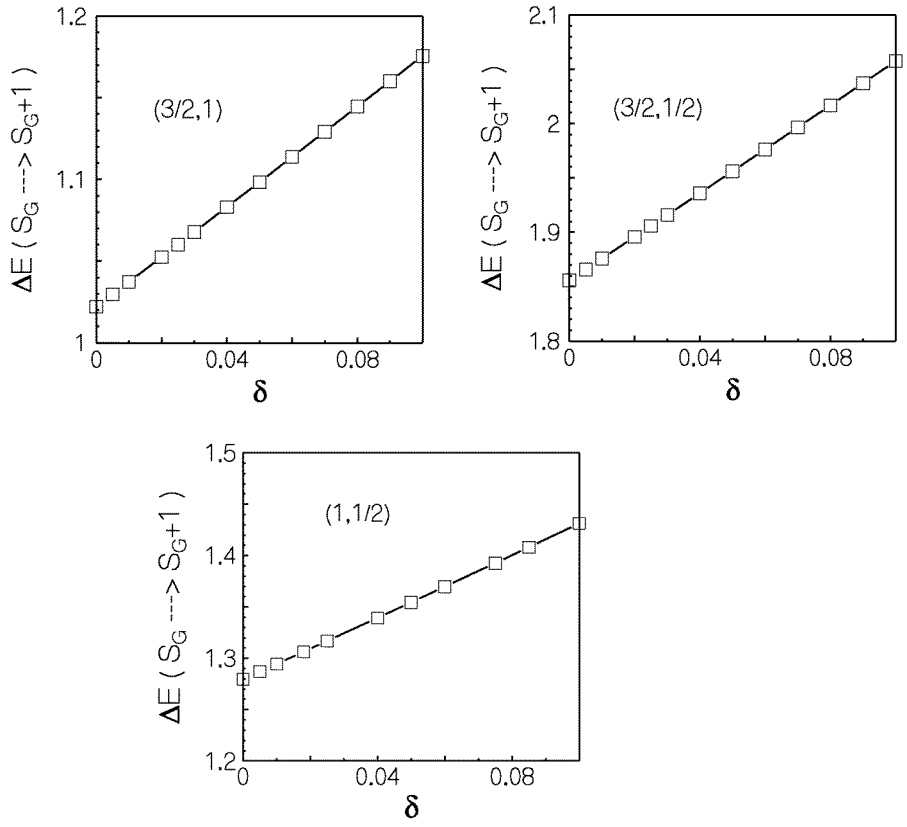

Figure 9. Excitation gaps (in units of J) to the state with spin $s = s_G + 1$ from the ground state ($s = s_G$) as functions of δ for the dimerized alternating chain. The exponent is 1.0 ± 0.01 for all three systems.

defined in equation (1). We calculate the lowest spin excitation to the $s = s_G - 1$ state from the ground state. We find that the $s = s_G - 1$ state is gapless from the ground state for all values of δ. This result agrees with the spin-wave analysis of the general (s_1, s_2) chain. The systems remain gapless even while dimerized unlike the pure antiferromagnetic dimerized spin chains. There is a smooth increase of the spin excitation gap from the ground state to the $s = s_G + 1$ state with increasing δ for all three systems studied here. We have plotted this gap versus δ in figure 9. The gap shows almost a linear behaviour as a function of δ, with an exponent of 1.0 ± 0.01 for all three systems [20]. This seems to be an interesting feature of all ferrimagnets. The spin-wave analysis however shows that this excitation gap is independent of δ for the general (s_1, s_2) chain. The similar behaviours of these three alternating spin systems suggest that a ferrimagnet can be considered as a ferromagnet with small quantum fluctuations.

3. Low-temperature properties

In this section, we present the results of our DMRG calculations of the thermodynamic properties of the $(\frac{3}{2}, 1)$, $(\frac{3}{2}, \frac{1}{2})$ and $(1, \frac{1}{2})$ spin systems. The size of the system varies from

8 to 20 sites. We impose periodic boundary conditions to minimize finite-size effects with $\boldsymbol{S}_{1,N+1} = \boldsymbol{S}_{1,1}$, so that the number of sites equals the number of bonds. We set up the Hamiltonian matrices in the DMRG basis for all allowed S_z-sectors for a ring of $2N$ sites. We can diagonalize these matrices completely to obtain all of the eigenvalues in each of the S_z-sectors. As the number of DMRG basis states increases rapidly with increasing m, we retain a smaller number of dominant density matrix eigenvectors in the DMRG procedure, i.e., $50 \leqslant m \leqslant 65$, depending on the S_z-sector as well as the size of the system. We have checked the dependence of the properties (with m in the range $50 \leqslant m \leqslant 65$) for the system sizes that we have studied ($8 \leqslant 2N \leqslant 20$), and have confirmed that the properties do not vary significantly for the temperatures at which they are computed; this is true for all three systems. The above extension of the DMRG procedure is found to be accurate by comparing with exact-diagonalization results for small systems.

It may appear surprising that the DMRG technique which essentially targets a single state, usually the lowest energy state in a chosen S_z-sector, should provide accurate thermodynamic properties since these properties are governed by energy level spacings and not the absolute energy of the ground state. However, there are two reasons for the DMRG procedure yielding reasonable thermodynamic properties at low temperatures. Firstly, the projection of the low-lying excited-state eigenfunctions on the DMRG space which contains the ground state is substantial; hence these excited states are well described in the chosen DMRG space. Secondly, the low-lying excitations of the full system are often the lowest energy states in different sectors in the DMRG procedure; hence their energies are quite accurate even on an absolute scale.

The canonical partition function Z for the $2N$-site ring can be written as

$$Z = \sum_j \mathrm{e}^{-\beta(E_j - B(M)_j)} \tag{8}$$

where the sum is over all of the DMRG energy levels of the $2N$-site system in all of the S_z-sectors. E_j and $(M)_j$ denote the energy and the $\hat{z}$-component of the total spin of the state j, B is the strength of the magnetic field in units of $J/g\mu_B$ (g is the gyromagnetic ratio and μ_B is the Bohr magneton) along the $\hat{z}$-direction, and $\beta = J/k_BT$ with k_B and T being the Boltzmann constant and temperature respectively. The field-induced magnetization $\langle M \rangle$ is defined as

$$\langle M \rangle = \left(\sum_j (M)_j \mathrm{e}^{-\beta(E_j - B(M)_j)} \right) \Big/ Z. \tag{9}$$

The magnetic susceptibility χ is related to the fluctuation in magnetization

$$\chi = \beta[\langle M^2 \rangle - \langle M \rangle^2]. \tag{10}$$

Similarly, the specific heat C is related to the fluctuation in the energy and can be written as

$$C = \frac{\beta}{T}[\langle E^2 \rangle - \langle E \rangle^2]. \tag{11}$$

The dimensionalities of the DMRG Hamiltonian matrices that we completely diagonalize vary from 3000 to 4000, depending upon the DMRG parameter m and the S_z-value of the targeted sector, for rings of sizes greater than 12. These matrices are not very sparse, owing to the cyclic boundary condition imposed on the system. The DMRG properties compare very well with exact results for small system sizes amenable to exact-diagonalization studies. In the discussion to follow, we present results on the 20-site ring although all calculations have been carried out for system sizes from 8 to 20 sites. This is because the qualitative

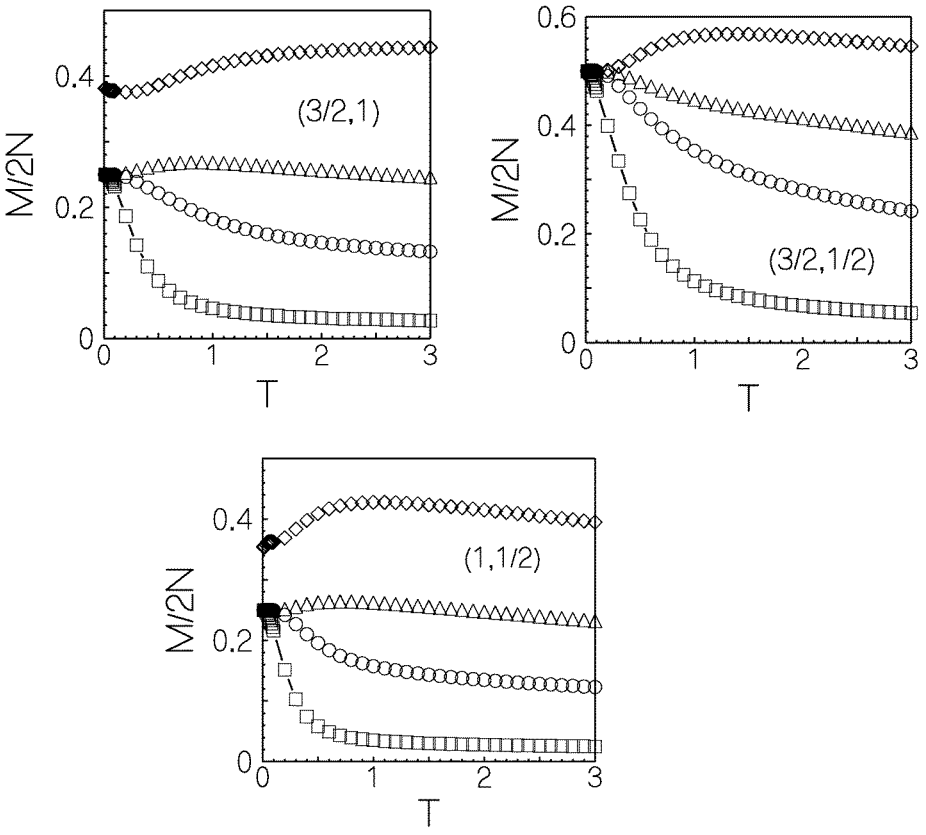

Figure 10. Plots of the magnetization per site as a function of temperature T for four different values of the magnetic field B. Squares are for $B = 0.1J/g\mu_B$, circles for $B = 0.5J/g\mu_B$, triangles for $B = J/g\mu_B$ and diamonds for $B = 2J/g\mu_B$.

behaviours of the properties that we have studied are similar for all of the ring sizes in this range for all three systems.

We present the dependence of magnetization on temperature for different magnetic field strengths in figure 10 for all three systems. At low magnetic fields, the magnetization shows a sharp decrease at low temperatures and shows paramagnetic behaviour at high temperatures. As the field strength is increased, the magnetization shows a slower decrease with temperature, and for high field strengths the magnetization shows a broad maximum. This behaviour can be understood from the type of spin excitation present in these systems. The lowest energy excitation at low magnetic fields is to a state with spin s less than s_G. Therefore, the magnetization initially decreases at low temperatures. As the field strength is increased, the gap to spin states with $s > s_G$ decreases as the Zeeman coupling to these states is stronger than that to the states with $s \leqslant s_G$. The critical field strengths at which the magnetization increases with temperature varies from system to system since this corresponds to the lowest spin gap of the corresponding system. The behaviour of the system at even stronger fields turns out to be remarkable. The magnetization in the ground state ($T = 0$) shows an abrupt increase signalling that the ground state at this field strength has $S_z > s_G$. The temperature dependence of the magnetization shows a broad maximum

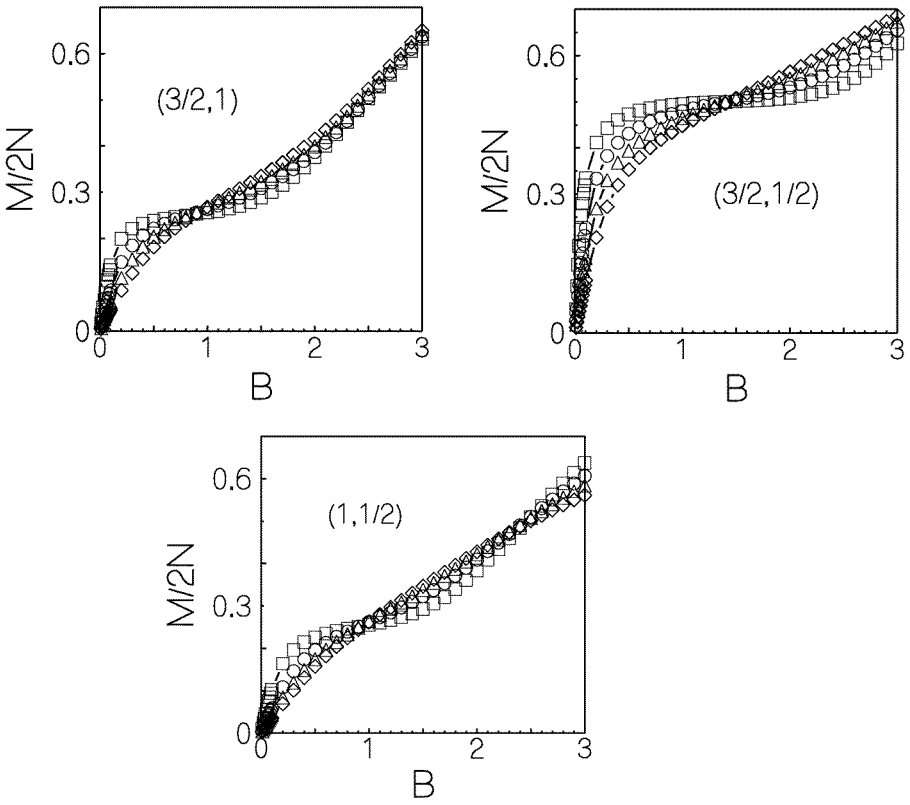

Figure 11. The magnetization per site versus the magnetic field strength B, in units of $J/g\mu_B$, for four different temperatures T. $T = 0.3J/k_B$ results are given by squares, $T = 0.5J/k_B$ results by circles, $T = 0.7J/k_B$ results by triangles and $T = J/k_B$ results by diamonds.

indicating the presence of states with even higher spin values lying above the ground state in the presence of this strong field. In all three cases, the ground state at very high field strengths should be ferromagnetic. For the systems at such high fields, the magnetization decreases slowly with increase of temperature as no other higher spin states lie above the ground state. While, we have not studied such high-field behaviours, we find that the field strength corresponding to switching the spin of the ground state s_G to $s_G + 1$ is higher for the $(\frac{3}{2}, \frac{1}{2})$ system as compared to the $(\frac{3}{2}, 1)$ and $(1, \frac{1}{2})$ systems. The switching field appears to depend on the value of $|s_1 - s_2|$. We see in figure 10 that in the $(\frac{3}{2}, 1)$ and $(1, \frac{1}{2})$ cases, the ground state has switched to the higher spin state at the highest magnetic field strength that we have studied, but in the $(\frac{3}{2}, \frac{1}{2})$ case, the ground state has not switched even at that field strength, indicating that the excitation gap for this system is larger than those for the other two. For the $(\frac{3}{2}, \frac{1}{2})$ case, the same situation should occur at very high magnetic fields. Thus, we predict that the highest s_z is attained in the ground state at high magnetic field and that this field strength increases with increase in site spin difference $|s_1 - s_2|$.

The dependence of the magnetization on the magnetic field is shown at different temperatures in figure 11 for all three systems studied here. At low temperature the magnetization shows a plateau. The width of the plateau depends on the system and it decreases as the temperature is raised. Eventually the plateau disappears at higher

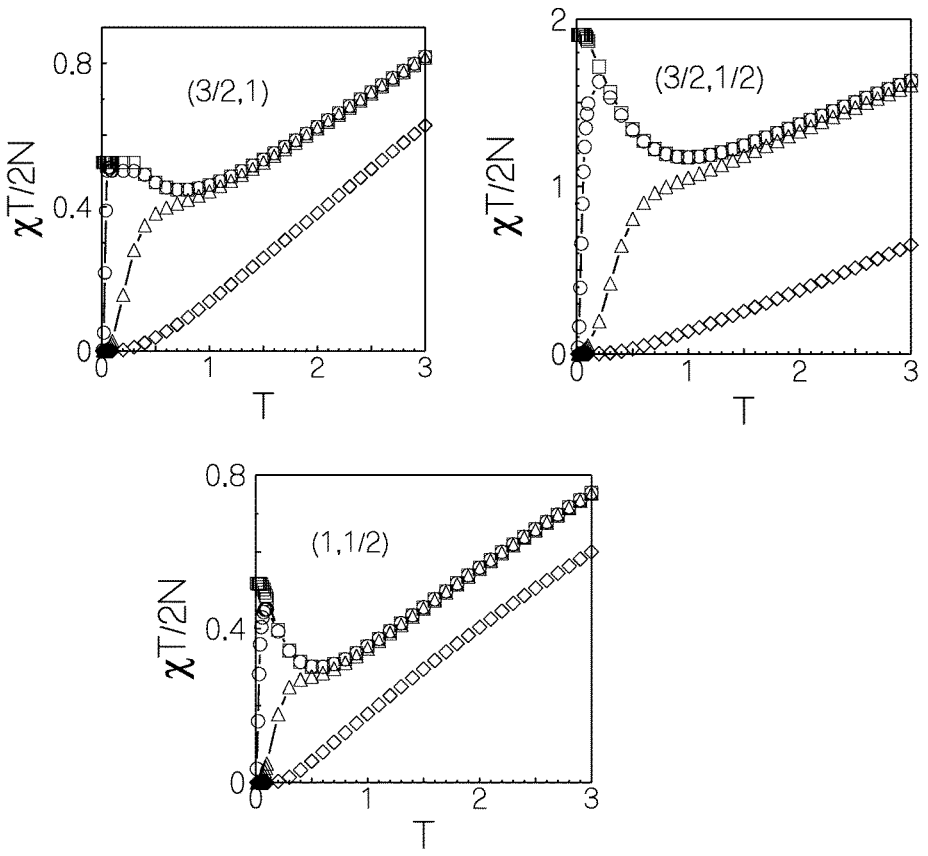

Figure 12. χT (defined in the text) per site as a function of temperature T for various magnetic fields B. Zero-field results are shown by squares, $B = 0.01J/g\mu_B$ results by circles, $B = 0.1J/g\mu_B$ results by triangles and $B = J/g\mu_B$ results by diamonds.

temperatures. The existence of the plateau shows that the higher spin states are not accessible at the chosen temperature. The plateau is widest in the $(\frac{3}{2}, \frac{1}{2})$ case, once again reflecting the larger gap to the s_G+1 state in this system compared with the $(\frac{3}{2}-1)$ and $(1, \frac{1}{2})$ systems. At higher fields, the larger Zeeman splittings of higher spin states become accessible, leading to an increase in the magnetization. The magetization curves at all temperatures intersect at certain field strengths depending on the system. For the $(\frac{3}{2}, 1)$ case, the intersection occurs at $B = 1.0J/g\mu_B$, and at higher field strengths all of the curves collapse. For the $(\frac{3}{2}, \frac{1}{2})$ case, the intersection occurs at $B = 1.5J/g\mu_B$, while for the $(1, \frac{1}{2})$ system these curves intersect twice, once at $B = 1.0J/g\mu_B$ and again at $B = 2.5J/g\mu_B$ in the chosen field range. These fields are close to the field strengths at which the ground state switches from one S_z-value to a higher value for the corresponding system. Thus, they are strongly dependent upon the actual values of s_1 and s_2.

The dependences of $\chi T/2N$ on temperature for different field strengths are shown in figure 12 for all three systems. For zero field, the zero temperature value of χT is infinite in the thermodynamic limit; for finite rings it is finite and equal to the average of the square of the magnetization in the ground state. For the ferrimagnetic ground state $\chi T/2N$, as $T \to 0$, is given by $s_G(s_G+1)/6N$. As the temperature increases, this product

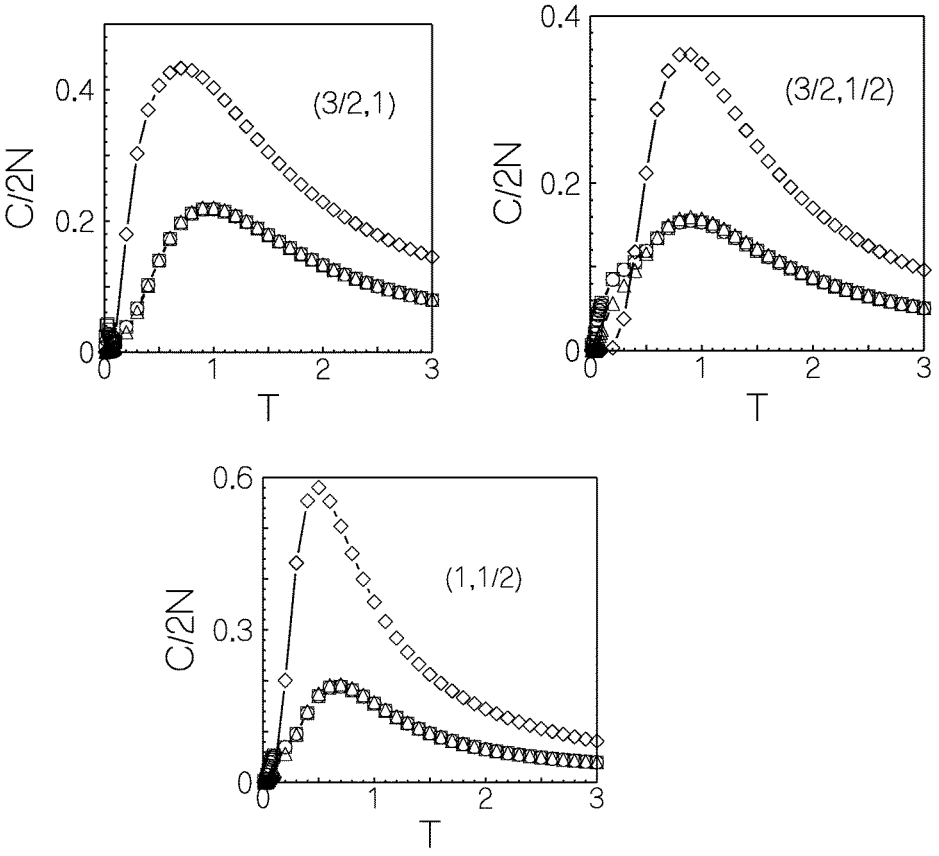

Figure 13. Specific heat per site as a function of temperature T for four different values of the magnetic field B. Zero-field data are shown by squares, $B = 0.01J/g\mu_B$ data by circles, $B = 0.1J/g\mu_B$ data by triangles and $B = J/g\mu_B$ data by diamonds.

decreases and shows a minimum before increasing again. For the three systems studied here, the minimum occurs at different temperatures depending on the system. For the $(\frac{3}{2}, 1)$ alternating spin system, it is at $k_BT = (0.8 \pm 0.1)J$, while for the $(\frac{3}{2}, \frac{1}{2})$ and $(1, \frac{1}{2})$ cases, it occurs at $k_BT = (1.0 \pm 0.1)J$ and $k_BT = (0.5 \pm 0.1)J$ respectively. The minimum occurs due to the states with $S_z < s_G$ getting populated at low temperatures. In the infinite-chain limit, these states turn out to be the gapless excitations of the system. The subsequent increase in the product χT is due to the higher-energy–higher-spin states being accessed with further increase in temperature. This increase is slow in the $(\frac{3}{2}, \frac{1}{2})$ case, as in this system very high spin states are not accessible within the chosen temperature range. Experimentally, it has been found in the bimetallic chain compounds that the temperature at which the minimum occurs in the χT-product depends upon the magnitude of the spins s_1 and s_2 [14]. The Ni^{II}–Cu^{II} bimetallic chain shows a minimum in $\chi T/2N$ at a temperature corresponding to 55 cm^{-1} (80 K); an independent estimate of the exchange constant in this system is 100 cm^{-1} [21]. This is in very good agreement with the minimum found theoretically at the temperature $(0.5 \pm 0.1)J$ for the $(1, \frac{1}{2})$ case. The minimum in $\chi T/2N$ vanishes at $B = 0.1J/g\mu_B$ which corresponds to about $10T$ for all three systems. It would be interesting to study the magnetic susceptibility of these systems experimentally under

such high fields. The low-temperature zero-field behaviour of our systems can be compared with that of the one-dimensional ferromagnet. In the latter, the spin-wave analysis shows that the χT-product increases as $1/T$ at low temperatures [22].

In finite but weak fields, the behaviour of χT is different. The magnetic field opens up a gap and χT falls exponentially to zero for temperatures less than the gap in the applied field for all three systems. Even in this case a minimum is found at the same temperature as in the zero-field case for the corresponding system, for the same reason as was discussed for the zero-field case.

In stronger magnetic fields, the behaviour of χT from zero temperature up to $k_B T = J_{min}$ (J_{min} is the temperature at which the minimum in χT is observed) is qualitatively different. The minimum in this case vanishes for all three systems. For these field strengths, the states with higher S_z-values are accessed even below $k_B T = J_{min}$. The dependence of χT above $k_B T = J_{min}$ at all field strengths is the same in all three systems. In even stronger magnetic fields, the initial sharp increase is suppressed. At very low temperature, the product χT is nearly zero and increases almost linearly with T over the temperature range that we have studied. This can be attributed to a switch in the ground state at this field strength. The very high-temperature behaviour of χT should be independent of field strength and should saturate to the Curie law value corresponding to the mean of the magnetic moments due to spin-s_1 and spin-s_2.

The temperature dependence of the specific heat also shows a marked dependence on the magnetic field at strong fields. This dependence is shown in figure 13 for various field strengths for all three systems. In zero and weak magnetic fields, the specific heat shows a broad maximum at different temperatures which are specific to the system. Interestingly, the temperature at which the specific heat shows a maximum closely corresponds to the temperature at which the low-field χT has a minimum for the corresponding system. For a strong magnetic field ($B = J$), there is a dramatic increase in the peak height at about the same temperature corresponding to the specific system, although the qualitative dependence is still the same as at low magnetic fields in all three cases. This phenomenon indicates that the higher-energy high-spin states are brought to within $k_B T$ of the ground state at this magnetic field strength for all three cases.

Studies of the thermodynamic properties of the dimerized alternating spin chains in these three cases show qualitatively similar trends to that of the corresponding uniform systems, and this follows from the fact that the low-energy spectrum does not change qualitatively upon dimerization.

4. Summary

We have studied alternating spin-$\frac{3}{2}$/spin-1 and spin-$\frac{3}{2}$/spin-$\frac{1}{2}$ systems in detail and compared them with our earlier studies on the spin-1/spin-$\frac{1}{2}$ model. The ground state and low-lying excited states have been analysed by employing the DMRG method and have been compared with the corresponding spin-wave results. The spin of the ground state is given by $s_G = N(s_1 - s_2)$ for a $2N$-site system in all three cases. There are two types of spin excitation in all of the systems. The lowest excitation one is gapless in the infinite-chain limit to a state with spin $s_G - 1$. Another excitation to the state with spin $s_G + 1$ is gapped and the gap is larger when the difference in site spins $|s_1 - s_2|$ is an integer. Interestingly, the low-energy spectrum remains qualitatively unchanged upon dimerization, and the dimerization is itself conditional in the infinite-chain limit for all three systems.

We have also employed the DMRG technique to obtain low-temperature thermodynamic

properties. For all of these cases, the magnetic susceptibility shows very interesting magnetic field dependence. The χT versus T plot shows a minimum at low magnetic fields, and the minimum vanishes at high magnetic fields. The temperature at which this minimum occurs varies from system to system. The specific heat shows a maximum as a function of temperature at all fields. Moreover, the height of the maximum shows a dramatic increase at high magnetic field. Interestingly, in each system, the temperature corresponding to the maximum in C and minimum in χT is the same at low magnetic fields.

Acknowledgments

We thank Professor Olivier Kahn who introduced one of us (SR) to the experimental alternating spin systems and thereby motivated us to undertake this work. The present work was supported by the Indo-French Centre for the Promotion of Advanced Research through project No 1308-4, 'Chemistry and Physics of Molecule-based Materials'.

References

[1] Fleming R M, Ramirez A P, Rosseinsky M J, Murphy D W, Haddon R C, Zahurak S M and Makhija A V 1991 *Nature* **352** 787
[2] Allemand P, Khemani K C, Koch A, Wudl F, Holczer K, Donovan S, Gruner G and Thompson J E 1991 *Science* **253** 301
[3] Miller J S, Epstein A J and Reiff W M 1988 *Chem. Rev.* **88** 201
[4] Ovchinnikov A A 1978 *Theor. Chim. Acta* **47** 297
[5] Ramasesha S, Sinha B and Albert I D L 1990 *Phys. Rev.* B **42** 9088
Sinha B and Ramasesha S 1993 *Phys. Rev.* B **48** 16 410
Miller J S and Dougherty D A 1989 *Proc. Symp. on Ferromagnetic and High-Spin Molecular Based Materials; Mol. Cryst. Liq. Cryst.* **176**
[6] For a review, see
Steiner M, Villain J and Windsor C G 1976 *Adv. Phys.* **25** 88
[7] Kahn O 1987 *Struct. Bonding* **68** 89
Kahn O 1993 *Molecular Magnetism* (New York: VCH)
[8] Kahn O, Pei Y, Verdaguer M, Renard J P and Sletten J 1988 *J. Am. Chem. Soc.* **110** 782
Van Koningsbruggen, Kahn O, Nakatani K, Pei Y, Renard J P, Drillon M and Leggol P 1990 *Inorg. Chem.* **29** 3325
[9] de Vega H J and Woynarovich F 1992 *J. Phys. A: Math. Gen.* **25** 4499
de Vega H J, Mezincescu L and Nepomechie R I 1994 *Phys. Rev.* B **49** 13 223
Aladin S R and Martins M J 1993 *J. Phys. A: Math. Gen.* **26** L529
Martins M J 1993 *J. Phys. A: Math. Gen.* **26** 7301
[10] Alcaraz F C and Malvezzi A L 1997 *J. Phys. A: Math. Gen.* **30** 767
Dörfel B-D and Meissner St 1997 *J. Phys. A: Math. Gen.* **30** 1831
[11] Kolezhuk A K, Mikeska H-J and Yamamoto S 1997 *Phys. Rev.* B **55** 3336
Brehmer S, Mikeska H-J and Yamamoto S 1997 *J. Phys.: Condens. Matter* **9** 3921
[12] Niggemann H, Uimin G and Zittartz J 1997 *Preprint* cond-mat/9703206
[13] Pati S K, Ramasesha S and Sen D 1997 *Phys. Rev.* B **55** 8894
[14] Kahn O 1995 *Adv. Inorg. Chem.* **43** 179
[15] White S R 1992 *Phys. Rev. Lett.* **69** 2863
White S R 1993 *Phys. Rev.* B **48** 10 345
[16] White S R and Huse D A 1993 *Phys. Rev.* B **48** 3844
Sorenson E S and Affleck I 1994 *Phys. Rev.* B **49** 15 771
[17] Hallberg K A, Horsch P and Martinez G 1995 *Phys. Rev.* B **52** R719
Bursill R J, Xiang T and Gehring G A 1994 *J. Phys. A: Math. Gen.* **28** 2109
Kato Y and Tanaka A 1994 *J. Phys. Soc. Japan* **63** 1277
[18] Chitra R, Pati S K, Krishnamurthy H R, Sen D and Ramasesha S 1995 *Phys. Rev.* B **52** 6581
Pati S K, Chitra R, Sen D, Krishnamurthy H R and Ramasesha S 1996 *Europhys. Lett.* **33** 707
[19] Schulz H J 1986 *Phys. Rev.* B **34** 6372

Affleck I, Gepner D, Schulz H J and Ziman T 1989 *J. Phys. A: Math. Gen.* **22** 511
Guo D, Kennedy T and Mazumdar S 1990 *Phys. Rev.* B **41** 9592
[20] Earlier extrapolation in the $(1, \frac{1}{2})$ case was done over the range of δ from 0 to 0.6. The present extrapolations are for the range of δ from 0 to 0.1, and hence there is a small difference from the earlier quoted value of 1.07 in reference [13].
[21] Kahn O 1996 private communication
[22] Takahashi M 1987 *Phys. Rev.* B **36** 3791